CHAPTER II
THEORETICAL BACKGROUND AND LITERATURE REVIEW

2.1 Phenol

2.1.1 General Remarks

Phenol is closely related to alcohols because of the presence of the hydroxyl (–OH) group. In phenol, however, the hydroxyl group is directly bonded to benzene ring. Phenolic compounds often have useful properties. Some are found in preservatives or medications. The chemistry of phenol is different than that of alcohols. Concentrated solutions of the phenol compound are quite toxic and can cause severe burns. Phenol is a common industrial chemical that is used in the manufacture of resins, plastics, fibers, adhesives, iron, steel, aluminum, leather, and rubber. It is also found in disinfectants, cleaners, cigarette smoke, and motor vehicle emissions (HSDB, 1991).

Classification of phenol compounds is divided into three types according to the number of phenol rings that are available.

1. Monocyclic phenols have one phenol ring and are commonly found in plants, such as phenol, catechol, hydro-quinone and p-hydroxycinnamic.
2. Dicyclic phenols have two phenol rings, such as flavonoids and lignans.
3. Polycyclic phenols or polyphenols include lignins, catechol melanins, flavolans (condensed tannins).

Phenol and its vapors are corrosive and hazardous to the eyes, the skin, and the respiratory tract. Repeated or prolonged skin contact with phenol may cause dermatitis, or even second and third-degree burns due to phenol caustic and deflating properties. Inhalation of phenol vapor may cause lung edema. The substance may cause harmful effects on the central nervous system and heart, resulting in dysrhythmia, seizures, and coma. The kidneys may be affected as well. Exposure may result in death, and the effects may be delayed. Long-term or repeated

exposure of the substance may have harmful effects on the liver and kidneys. The toxic, acute, and chronic effects of phenol are shown in Table 2.1.

Table 2.1 The toxic, acute, and chronic effects of phenol (http://ehs.ucla.edu/SOP/Sodium_Azide.doc)

Toxic effects	Phenol is a toxic substance. Phenol is a poison and toxic via ingestion, inhalation, and skin absorption. This chemical is easily absorbed through the skin, and fatalities have been documented from skin absorption through a relatively small surface area.
Acute effects	Acute phenol intoxication causes shock, collapse, coma, convulsions, cyanosis, and death. Ingestion of lethal amounts causes severe burns of the mouth and throat, marked abdominal pain, cyanosis, muscular weakness, collapse, coma, and death. Tremors, convulsions, and muscle twitching have also occurred. Contact of the skin with the solid or liquid can produce chemical burns, redness, edema, tissue necrosis, and gangrene; contact with the eye may result in irritation, conjunctival swelling, whitened cornea, and blindness.
Chronic effects	Chronic phenol poisoning is characterized by vomiting, difficult swallowing, excessive salivation, diarrhea, anorexia, headache, fainting, vertigo, mental disturbances, and possibly skin eruptions. Prolonged cutaneous exposure may result in deposition of dark pigment in the skin.

2.2 Semiconductor

A semiconductor is a material with an electrical conductivity that is intermediate between that of an insulator and a conductor. Like other solids, semiconductor materials have electronic band structure determined by the crystal properties of the material. A semiconductor used as photocatalyst should be an oxide or sulfide of metals, such as TiO_2, CdS, and ZnO. The actual energy distribution among electrons is described by the Fermi level and temperature of the electrons. At absolute zero temperature, all of the electrons have energy below the Fermi energy, but at non-zero temperature, the energy levels are randomized, and some electrons have energy above the Fermi level.

Among the bands filled with electrons, the one with the highest energy level is referred to as the valence band, and the band outside of this is referred to as the conduction band. The energy width of the forbidden band between the valence band and the conduction band is referred to as the band gap. The overall structure of band gap energy is shown in Figure 2.1

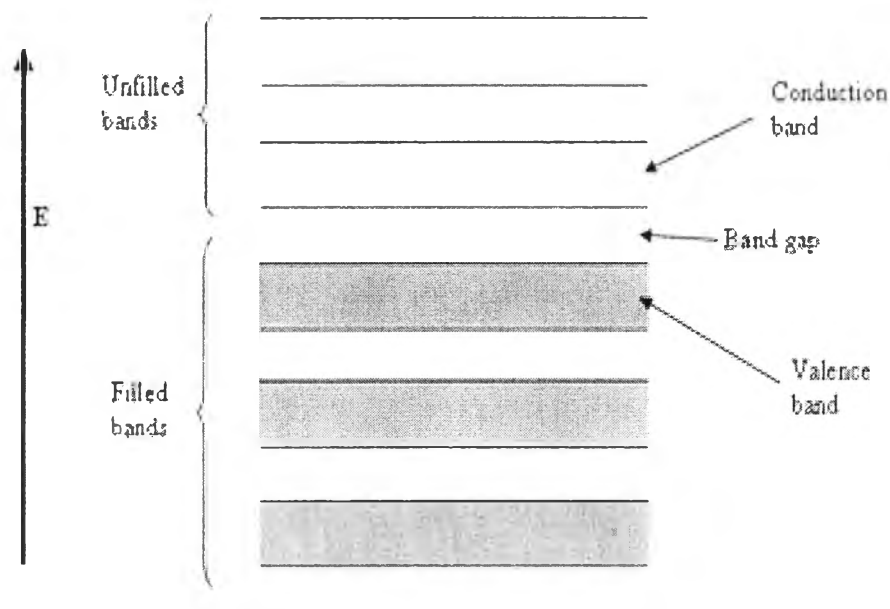

Figure 2.1 The structure of band gap energy.

The band gap can be considered as a wall that electrons must jump over in order to become free. The amount of energy required to jump over the wall is referred to as the band gap energy (E_g). Only electrons that jump over the wall and enter the conduction band (CB), which are referred to as conduction band electrons, can move around freely. When light is illuminated at appropriate wavelengths with energy equal or more than band gap energy, valence band (VB) electrons can move up to the conduction band (CB). At the same time, as many positive holes as the number of electrons that have jumped to the conduction band (CB) are created. The valence band (VB), conduction band (CB), band gap, and band gap wavelength of some common semiconductors are shown in Table 2.2

Table 2.2 The band gap positions of some common semiconductor photocatalysts (Robertson, 1996)

Semiconductor	Valence band (eV)	Conduction band (eV)	Band gap (eV)	Band gap wavelength (nm)
TiO_2	+3.1	-0.1	3.2	387
SnO_2	+4.1	+0.3	3.8	326
ZnO	+3.0	-0.2	3.2	387
ZnS	+1.4	-2.3	3.7	335
WO_3	+3.0	+0.2	2.8	443
CdS	+2.1	-0.4	2.5	496
CdSe	+1.6	-0.1	1.7	729
GaAs	+1.0	-0.4	1.4	886
GaP	+1.3	-1.0	2.3	539

Wide band gap semiconductors, such as oxides (TiO_2, ZnO, WO_3, and Fe_2O_3) and chalcogenides (commonly CdS), are commonly employed as photocatalyst in heterogeneous photocatalysis, of which it involves electron-hole pair formation initiated by band gap excitation of a semiconductor particle. Upon photoexcitation of several semiconductors inhomogeneously suspended in either

aqueous or gaseous mixtures, simultaneous oxidation and reduction reactions occur. Molecular oxygen is often assumed to serve as the oxidizing agent. Heterogeneous photocatalytic processes can be defined as catalytic processes, during which one or more reaction steps occur by means of electron-hole (e^--h^+) pairs photogenerated on the surface of semiconductor materials illuminated by light of suitable energy. Some steps of a photocatalytic process are redox reactions, involving the photogenerated electron-hole pairs (Amar, 2007). The detail of the photocatalytic degradation processes will be described later.

2.3 Photocatalyst

2.3.1 Titanium Dioxide (TiO_2)

Titanium dioxide (TiO_2) is a wide band gap semiconductor that has been extensively investigated and applied to a wide spectrum of chemical disciplines. Its uses are, for instances, in selective oxidation and reduction, polymerization, condensation reaction, substitutional fluorination of olefins and phosphates, photovoltaics, and in photodegradation of organic and inorganic compounds (Fox and Chen, 1981). The high photoactivity, thermal and chemical stability, low cost, and non-toxicity of TiO_2 make it a good candidate for such applications. TiO_2 is found in three crystalline phases: anatase, rutile, and brookite, as well as in an amorphous phase. The anatase phase has a band gap energy of 3.2 eV, the rutile phase of 3.0 eV, and the brookite phase of 3.4 eV at room temperature. (Hoffmann *et al.*, 1995). This corresponds to maximal wavelength absorptions ranging from 365 to 413 nm. Upon illumination of the TiO_2 with light of equal or greater energy than its band gap energy, charge transfer from valence band to conduction band occurs, creating a hole (h^+) and a free electron (e^-). These species can either recombine or migrate to the surface and react with surface-bound adsorbates, typically oxygen or water in most photo-oxidative processes. Since UV light makes up of less than 5 % of the solar spectrum that reaches the earth's surface, the commercial application of these processes has been limited. However, a large degree of characterization works has been accomplished to date.

The main four polymorphs of TiO_2 found in nature are anatase (tetragonal), brookite (orthorhombic), rutile (tetragonal), and TiO_2 (B) (monoclinic). The structures of rutile, anatase, and brookite can be discussed in terms of (TiO_2^{6-}) octahedrals. The three crystal structures differ by the distortion of each octahedral and by the assembly patterns of the octahedral chains. Anatase can be regarded to be builtup from octahedrals that are connected by their vertices; in rutile, the edges are connected; and in brookite, both vertices and edges are connected, as shown in Figure 2.2 (Carp *et al.*, 2004).

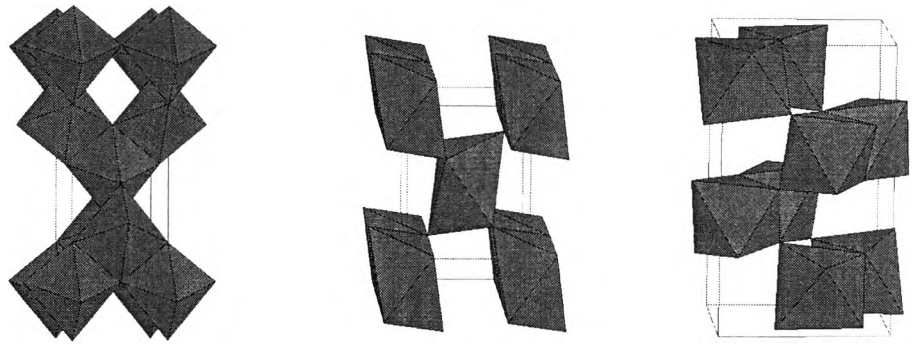

(a) (b) (c)

Figure 2.2 Crystal structures of (a) anatase, (b) rutile, and (c) brookite.

In photocatalysis applications, both crystal structures, i.e. anatase and rutile, are commonly used, with anatase showing a greater photocatalytic activity for most reactions. It has been suggested that this increased photoreactivity is due to anatase's slightly higher Fermi level, lower capacity to adsorb oxygen, and higher degree of hydroxylation (i.e. number of hydroxyl groups on the surface). Reactions, in which both crystalline phases have the same photoreactivity (Deng *et al.*, 2002) or rutile a higher one (Mills *et al.*, 2003), are also reported. Furthermore, there are also studies, which claim that a mixture of anatase (70-75 %) and rutile (30-25 %) is more active than pure anatase (Mugglie and Ding, 2001). The disagreement of the results may lie in the intervening effect of various coexisting factors, such as specific surface area, pore size distribution, crystal size, and preparation methods, or in the way the activity is expressed. The behavior of Degussa P-25 commercial TiO_2

photocatalyst, consisting of a mixture of anatase and rutile in an approximate proportion of 80/20, is for many reactions more active than both the pure crystalline phases. The enhanced activity arises from the increased efficiency of the e^-/h^+ separation due to the multiphase nature of the particles.

As a semiconductor, TiO_2 functions by having a large band gap, which can be described as an energy threshold that electrons must obtain in order to flow through a material. The band gap is located between the filled valence band and the higher energy conduction band. The magnitude between the electronically occupied valence band and the largely unpopulated conduction band determines both the extent of thermal population of the conduction band (i.e. the electrical conductivity of the material) and the wavelength sensitivity of the semiconductor to irradiation. That is, a material with a larger band gap requires higher energy radiation to populate the conduction band than one with a smaller band gap.

The general mechanism for photocatalytic reaction on semiconductor TiO_2 can be explained as shown in Figure 2.3. The absorption of light in TiO_2 at the wavelengths of less than 387 nm (for the anatase crystal with the band gap of 3.2 eV) leads to the promotion of an electron from the valence band to the conduction band of the semiconductor. This excitation process creates an electron in the conduction band and an electron vacancy (a hole) in a valence band. The electron-hole pairs that are generated in this way migrate toward the surface where they can initiate the redox reactions with absorbates. Because the valence band edge of TiO_2 is located at approximately +3.2 eV with respect to a normal hydrogen electrode (NHE) at pH 0 (the position of the band edge is pH-dependent), these holes are very powerful oxidizing agents and are capable of oxidizing a variety of organic molecules, leading to the formation of mainly CO_2 and H_2O. However, the main issue to be taken into consideration is that TiO_2 photocatalyst can only be exited by UV light because of their wide band gap.

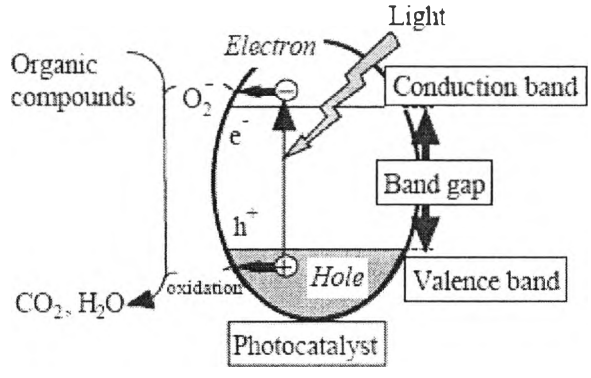

Figure 2.3 Mechanism of photocatalysis.

2.3.2 Doping of TiO_2

Noble metals, including Pt, Au, Pd, Rh, Ni, Cu and Ag, have been reported to be very effective for enhancement of TiO_2 photocatalysis. As the Fermi levels of these noble metals are lower than that of TiO_2, photo-excited electrons can be transferred from conduction band to metal particles deposited on the surface of TiO_2, while photo-generated valence band holes remain on the TiO_2. These activities greatly reduce the possibility of electron-hole recombination, resulting in efficient separation and stronger photocatalytic reactions. As electrons accumulate on the noble metal particles, their Fermi levels shift closer to the conduction band of TiO_2, resulting in more negative energy levels. This is beneficial for water splitting for hydrogen production. Furthermore, smaller metal particles deposited on TiO_2 surface exhibit more negative Fermi level shift. Accumulated electrons on metal particles can then be transferred to protons adsorbed on the surface and further reduce the protons to hydrogen molecules. Therefore, noble metals with suitable work function can help electron transfer, leading to higher photocatalytic activity.

The influence of metal doping on the photocatalytic was investigated Zhu *et al.* (2006). It was found that the optimum dopant concentration for Fe^{3+}-modified TiO_2 is 0.15 at%. Doping of Fe^{3+} was affirmed to introduce much more oxygen vacancies, which favored the adsorption of water and formation of surface hydroxyl group. The Cu doping on TiO_2 was also investigated by Wong *et al.* (2005) The 100% color removal and 99% TOC removal of 0.2 mM acid orange 7 (AO7)

after 15 min reaction were achieved. Moreover, Sung-Suh *et al.* (2004) used the optimum 2 at.% Ag doping on TiO_2 to achieve the highest efficiency of the rhodamine B (RB) photodegration.

2.3.3 Co-modification of Photocatalyst

Powders with semiconductor characteristics have been widely employed in photocatalytic systems because they are capable of generating charge carriers by absorbing photon energies. The separation effectiveness of the photo-induced charge carriers is an important factor in determining the photocatalytic activity of the powders. One promising photocatalyst is perovskite-related material. Perovskite-related materials are represented by the general formula of ABO_3 (A = rare earth and alkali element with or without its partial substitution by alkaline earth element, and B = transition element, such as Co, Mn, Ti, Ta, Ni, Fe, etc., with or without its partial substitution) (Hu *et al.*, 2007). The interest of these materials for the photochemical splitting of water derives from the possibility to use their interlayer space for reaction sites, where electron-hole recombination process could be retarded by physical separation of electron and hole pairs generated by photo-absorption.

When applied to semiconductor, the term *doping* refers to the intentional introduction of impurities to the material for the purpose of modifying electrical characteristics. With the above depiction of semiconduction in mind, an ideal dopant must increase the valence band edge, thus reducing the band gap without lowering the conduction band, and either improve or at least minimize electron-hole recombination, so as to minimize any loss in quantum yield. It also should not impart any instability, have thermal or chemical stability, and optimally be inexpensive to apply.

A number of methods have been investigated and found to narrow the band gap of TiO_2. A common method, used successfully for solar cell applications, is accomplished by attaching various organic dyes, such as ruthenium complexes, to the surface (Hoffmann *et al.*, 1995). Unfortunately, this method is expensive, and such dyes degrade in the presence of oxygen. Ruthenium dyes also cannot be used in aqueous solutions as they can be readily washed off from the surface. Reduction of

TiO_2 via hydrogenation has also been investigated. This method does narrow the band gap, allowing visible light for activation, but at the expense of lowering the conduction band, thus reducing the photocatalytic reduction power of the system. Another method available to narrow the band gap is to dope the semiconductor with metals and non-metals. Most transition and rare earth metals have been investigated. Metals, such as Fe^{3+}, Mo^{5+}, Rh^{3+}, V^{4+}, and Ru^{3+} have been found to tune the electronic structure of TiO_2 and improve its photocatalytic activity in the visible range.

Puangpetch *et al.* (2008) investigated the use of a sol-gel method with the aid of structure-directing surfactant (LAHC, CTAB, and CTAC) for preparing mesoporous-assembled $SrTiO_3$ nanocrystals. The photocatalytic activity was investigated via the photodegradation of methyl orange as a model azo dye contaminant in a wastewater. The results showed that the use of EtOH a the solvent yielded a $SrTiO_3$ photocatalyst with a higher purity than ethylene glycol (EG) or EtOH/EG mixture. The $SrTiO_3$ with narrow pore size distribution was obtained when LAHC was used as the structure-directing surfactant. Besides, the surface area and pore size distribution could be controlled by adjusting molar ratio of LAHC to tetraisopropyl orthotitanate (TIPT). The highest photocatalytic activity of $SrTiO_3$ was achieved at the LAHC:TIPT ratio of 0.25:1 and calcination temperature of 700°C

Khunrattanaphon *et al.* (2011) investigated the synthesis of $SrTi_xZr_{1-x}O_3$ (x = 0-1) photocatalysts and photocatalytic activity in acid black (AB) diazo dye used as a model contaminant in textile wastewater. The effects of varying Ti-to-Zr molar ratio (as expressed by x in the $SrTi_xZr_{1-x}O_3$), calcination conditions, and Pt loading were investigated. The synthesized mesoporous-assembled $SrTi_{0.9}Zr_{0.1}O_3$ photo-catalyst was found to show a highest photocatalytic activity. In addition, under the optimum Pt loading of 1.0 wt.% at the calcination temperature of 850 °C, the photocatalytic degradation rate constant of $SrTi_{0.9}Zr_{0.1}O_3$ photocatalyst was significantly enhanced from 1.05 h^{-1} (without Pt loading) to 3.0 h^{-1}.

2.4 Nano-Photocatalysts

2.4.1 General Remarks

Nanocrystalline photocatalysts are ultra-small semiconductor particles, which are few nanometers in size. During the past decade, the photochemistry of nanosized semiconductor particles has been one of the fastest growing research areas in physical chemistry. The interest in these small semiconductor particles originates from their unique photophysical and photocatalytic properties. Several review articles have been published concerning the photophysical properties of nanocrystalline semiconductors. Such studies have demonstrated that some properties of nanocrystalline semiconductor particles are in fact different from those of bulk materials.

Nanosized particles possess properties with falling into the region of transition between the molecular and bulk phases. In the bulk material, the electron excited by light absorption funds a high density of states in the conduction band, where it can exist with different kinetics energies. In the case of nanoparticles, however, the particle size is the same as or smaller than the size of the first excited state. Thus, the electrons and holes generated upon illumination cannot suit into such a particle, unless they assume a state of higher kinetics energy.

Hence, as the size of the semiconductor particle is reduced below a critical diameter, the spatial confinement of the charge carriers within a potential well, like ''a particle in a box'', causes them to mechanically behave quantum. In solid state terminology, this means that the bands split into discrete electronic states (quantized levels) in the valence and conduction bands, and the nanoparticle progressively behaves similar to a giant atom. Nanosized semiconductor particles, which exhibit size-dependent optical and electronic properties, are called quantized particles or quantum dots (Kamat, 1995).

2.4.2 Activity of Nano-Photocatalysts

One of the main advantages of the application of nanosized particles is the increase in the band gap energy with decreasing particle size. As the size of a semiconductor particle falls below the critical radius, the charge carriers begin to

behave mechanically quantum, and the charge confinement leads to a series of discrete electronic states. As a result, there is an increase in the effective band gap and a shift of the band edges. Thus by varying the size of the semiconductor particles, it is possible to enhance the redox potential of the valence band holes and the conduction band electrons.

However, the solvent reorganizational free energy for charge transfer to a substrate remains unchanged. The increasing driving force and the unchanged solvent reorganizational free energy are expected to lead to an increase in the rate constants for charge transfer at the surface. The use of nanosized semiconductor particles may result in an increased photocatalytic activity for systems, in which the rate-limiting step is interfacial charge transfer. Hence, nanosized semiconductor particles can possess an enhanced photoredox chemistry with reduction reactions, which might not otherwise proceed in bulk materials, being able to occur readily using sufficiently small particles. Another factor, which could be advantageous, is the fact that the fraction of atoms that are located at the surface of a nanoparticle is very large. Nanosized particles also have high surface area-to-volume ratio, which further enhances their catalytic activity. One disadvantage of nanosized particles is the need for light with a shorter wavelength for photocatalyst activation. Thus, a smaller percentage of a polychromatic light source will be useful for photocatalysis.

In large TiO_2 particles (Zhang *et al.*, 1998), volume recombination of the charge carriers is the dominant process and can be reduced by a decrease in particle size. This decrease also leads to an increase in the surface area, which can be translated as an increase in the available surface active sites. Thus, a decrease in particle size should also result in higher photonic efficiencies due to an increase in the interfacial charge carrier transfer rates. However, as the particle size is lowered below a certain limit, surface recombination processes become dominant, since firstly most of the electrons and holes are generated close to the surface, and secondly surface recombination is faster than interfacial charge carrier transfer processes. This is the reason why there exists an optimum particle size for maximum photocatalytic efficiency.

2.5 Photocatalytic Decomposition Mechanisms

2.5.1 Photocatalytic Oxidation

It is well established that conduction band electrons (e^-) and valence band holes (h^+) are generated when aqueous TiO_2 suspension is irradiated by light with energy greater than its band gap energy (E_g, 3.2 eV). The photogenerated electrons can reduce the phenol or react with electron acceptors, such as O_2 adsorbed on the Ti(III)-surface or dissolved in water, reducing it to superoxide radical anion, $O_2^{\bullet-}$. The photogenerated holes can oxidize the organic molecule to form R^+ or react with OH^- or H_2O, oxidizing them into $OH^\bullet$ radicals. Together with other highly oxidant species (peroxide radicals), they are reported to be responsible for the heterogeneous TiO_2 photodecomposition of organic substrates, such as phenol. According to this, the relevant reactions at the semiconductor surface causing the decomposition of phenol can be expressed as follows:

$$TiO_2 + h\nu(UV) \rightarrow TiO_2(e_{CB}^- + h_{VB}^+) \quad (1)$$

$$TiO_2(h_{VB}^+) + H_2O \rightarrow TiO_2 + H^+ + OH^\bullet \quad (2)$$

$$TiO_2(h_{VB}^+) + OH^- \rightarrow TiO_2 + OH^\bullet \quad (3)$$

$$TiO_2(e_{CB}^-) + O_2 \rightarrow TiO_2 + O_2^{\bullet-} \quad (4)$$

$$O_2^{\bullet-} + H^+ \rightarrow HO_2^\bullet \quad (5)$$

$$\text{Phenol} + OH^\bullet, HO_2^\bullet, O_2^{\bullet-} \rightarrow \text{decomposition products} \quad (6)$$

$$\text{Phenol} + h_{VB}^+ \rightarrow \text{oxidation products} \quad (7)$$

$$\text{Phenol} + e_{CB}^- \rightarrow \text{reduction products} \quad (8)$$

The resulting $OH^\bullet$ radical, being a very strong oxidizing agent (standard redox potential of +2.8 V), as well as $HO_2^\bullet$ and $O_2^{\bullet-}$ can oxidize most of phenol to the mineral end-products. Substrates not reactive toward hydroxyl radicals are decomposed employing TiO_2 photocatalysis with rates of decay highly influenced by the semiconductor valence band edge position. The role of reductive pathways (Equation (8)) in heterogeneous photocatalysis has been envisaged also in the decomposition of several dyes but in a minor extent than oxidation.

2.5.2 Photosensitized Oxidation

The mechanism of photosensitized oxidation (called also photoassisted decomposition) by visible radiation (λ > 420 nm) is different from the pathway implicated under UV light radiation. In the former case, the mechanism suggests that excitation of the adsorbed phenol takes place by visible light to appropriate singlet or triplet states, subsequently followed by electron injection from the excited phenol molecule into the conduction band of the TiO_2 particles, whereas the phenol is converted to the cationic phenol radicals ($phenol^{\bullet+}$) that undergoes decomposition to yield products as follows:

$$phenol + hv(visible) \rightarrow phenol^* \quad (9)$$

$$phenol^* + TiO_2 \rightarrow phenol^{\bullet+} + TiO_2(e_{CB}^-) \quad (10)$$

$$TiO_2(e_{CB}^-) + O_2 \rightarrow O_2^{\bullet-} + TiO_2 \quad (11)$$

$$phenol^{\bullet+} \rightarrow \text{decomposition products} \quad (12)$$

The cationic phenol radicals readily react with hydroxyl ions, undergoing oxidation via Equations (13) and (14), or interact effectively with $O_2^{\bullet-}$, $HO_2^{\bullet}$, or $HO^{\bullet-}$ species to generate intermediates that ultimately lead to CO_2 (Equations (15) – (19)).

$$phenol^{\bullet+} + OH^- \rightarrow phenol + HO^{\bullet} \quad (13)$$

$$phenol + 2HO^{\bullet} \rightarrow H_2O + \text{oxidation products} \quad (14)$$

$$O_2^{\bullet-} + H^+ \rightarrow HO_2^{\bullet} \quad (15)$$

$$HO_2^{\bullet} + H^+ + TiO_2(e_{CB}^-) \rightarrow H_2O_2 + TiO_2 \quad (16)$$

$$H_2O_2 + TiO_2(e_{CB}^-) \rightarrow HO^{\bullet} + HO^- + TiO_2 \quad (17)$$

$$phenol^{\bullet+} + O_2^{\bullet-} \rightarrow DO_2 \rightarrow \text{decomposition products} \quad (18)$$

$$phenol^{\bullet+} + HO_2^{\bullet}(\text{or } HO^{\bullet}) \rightarrow \text{decomposition products} \quad (19)$$

When using sunlight or simulated sunlight (laboratory experiments), it is suggested that both photooxidation mechanisms occur during the irradiation, and both TiO_2 and the light source are necessary for the reaction to occur. In the photocatalytic oxidation, TiO_2 has to be irradiated and excited in a near-UV energy to induce charge separation.

A possible mechanism of phenol oxidation in presence of illuminated TiO_2 is shown in Figure 2.4 (Sobczynski *et al.*, 2004)

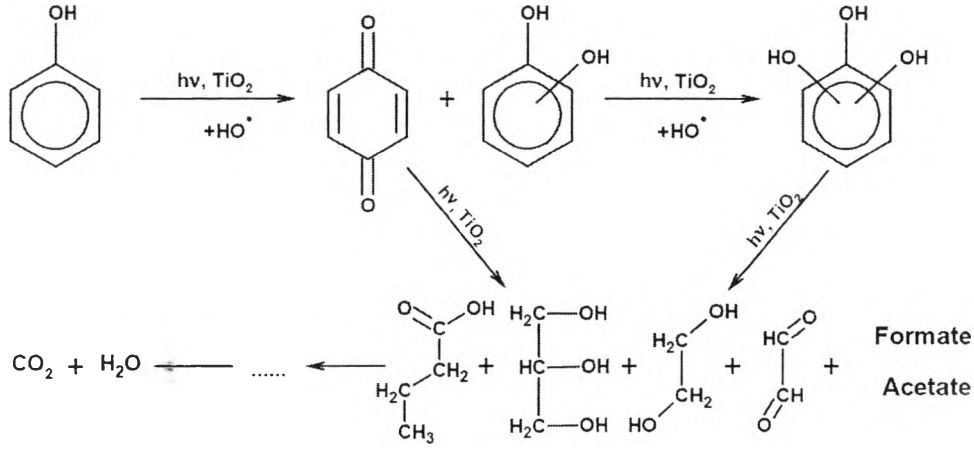

Figure 2.4 A possible mechanism of phenol degradation on illuminated TiO_2.

2.6 Factors Influencing the Photocatalytic Decomposition

2.6.1 Effect of Initial Phenol Concentration

Chiou *et al* (2008) studied the decomposition of phenol by TiO_2 (P-25). The results showed that with different initial phenol concentrations varied from 0.13 to 1.01 mM, the decomposition efficiency decreased with increasing concentration of phenol. The strong decrease in the observed rate constants with the increase in initial phenol concentration was attributed to the significant absorption of light by the substrate in the same wavelength range of photocatalyst excitation. For increasing the initial phenol concentration, more and more molecules of the compound get adsorbed on the surface of the photocatalyst. So, the requirement of reactive species ($OH^{\bullet}$ and $O_2^{\bullet-}$) needed for the degradation of pollutant also increases; however, the formation of reactive species remains constant. Therefore, the available $OH^{\bullet}$ species are inadequate for the pollutant degradation at higher concentrations. Thus, the degradation rate of pollutant decreases when the concentration increases. In addition, an increase in pollutant concentration can lead to the generation of intermediates, which may adsorb on the surface of the catalyst. Diffusion of intermediates from the catalyst surface can result in the deactivation of active site of the photocatalyst, and result in a decrease in the degradation rate (Ahmed *et al.*, 2010).

2.6.2 Effect of Solution pH

The heterogeneous photocatalysis has been found to be pH dependent. Chiou *et al* (2008) also showed that with different initial pH values (2.45, 3.96, 7.36, 8.94, 10.9, and 13.0), The photodegradation of phenol is not favored in an acidic solusion (pH < 3). An increase in solution pH enhances the photodegradation, and reaches a maximum at pH 7.4. However, photodegradation decreases when the pH further increases. At acidic to neutral media, phenol is primarily in its nonionic form; water solubility is minimized; and the adsorption onto the surface catalyst is maximized. On the other hand, phenol tends to exist as phenolate anions at higher pH values, and the anions have high solubility in solution and will not be adsorbed significantly. At a pH above 11, phenol is completely in the form of phenolate anion, and surface of TiO_2 will be negatively charged that should hinder the adsorption of negative charges.

2.6.3 Effect of Light Intensity and Irradiation Time

Oillis *et al.* (1991) reviewed the studies reported for the effect of light intensity on the kinetics of the photocatalysis process and stated that (i) at low light intensities (0–20 mW/cm^2), the rate would increase linearly with increasing light intensity (first order), (ii) at intermediate light intensities beyond a certain value (approximately 25 mW/cm^2), the rate would depend on the square root of the light intensity (half order), and (iii) at high light intensities, the rate is independent of light intensity. This is likely because at low light intensity, reactions involving electron–hole formation are predominant, and electron–hole recombination is negligible. However, when increasing light intensity, electron–hole pair separation competes with recombination, thereby causing lower effect on the reaction rate. It is evident that the percentage of decolorization and degradation increases with an increase in irradiation time. The reaction rate decreases with irradiation time since it follows apparent first-order kinetics, and additionally a competition for decomposition may occur between the reactant and the intermediate products. The slow kinetics of dye decomposition after certain time limit is due to:

- The difficulty in converting the N-atoms of dye into oxidized nitrogen compounds
- The slow reaction of short chain aliphatics with $OH^{\bullet}$ radicals
- The short life-time of photocatalyst

because of active site deactivation by strong by-product adsorption (Konstantinou and Albanis, 2004).

2.6.4 Effect of H_2O_2 Addition

The influence of the strong oxidant species additives, such as H_2O_2, has been in some case controversial, and it appeared strongly dependent on substrate type and on various experimental parameters. Their usefulness should be accurately checked under each operative condition.

Chiou *et al.* (2008) studied the decomposition of phenol and showed that with different concentrations of H_2O_2 (0, 1.77, 5.29, 8.82, 44.1 and 88.2 mM), when the H_2O_2 was added, a significant increase in decomposition rate was noted for phenol decomposition but must be in the presence of photocatalyst and light irradiation. Moreover, partial decomposition was observed for phenol under irradiation of the homogeneous systems in the presence of H_2O_2. The added H_2O_2 contributed to the reactive radical intermediates ($OH^{\bullet}$) formed from the oxidants by reaction with the photogenerated electrons, which can exert a dual function: as strong oxidant themselves and as electron scavengers, thus inhibiting the electron–hole recombination at the semiconductor surface.

2.6.5 Effect of Calcination Temperature of Photocatalyst

Yao *et al.* (2004) studied the effect of different calcination temperatures of photocatalyst for 5 min (400, 500, 600, and 700 °C) at the same concentration of methyl orange (10 mg/l). The results showed that the photocatalytic activity of photocatalyst had no significant difference among the calcination temperatures of 400, 500, and 600 °C, but the photocatalytic activity of the prepared photocatalysts was significantly reduced at higher calcination temperature (700 °C).

Zhang *et al.* (2004) studied the photocatalytic activity of $ZnO–SnO_2$ for decomposition of methyl orange, and the effect of heat treating at different calcination temperatures was investigated (300, 350, 400, 450, 500, 600, 700, 800, and 900 °C). The results showed that the degradation rate of methyl orange was increased with increasing calcination temperature, except for 300 °C because of the partial formation of crystallite oxides. With increasing calcination temperature, the size of crystallite oxides increases, contributing to the increase in photocatalytic activity. However, at temperatures higher than 700 °C, the photocatalyst exhibited poor activity because of the negative effect of the coupled oxides.

2.6.6 Effect of Calcination Time of Photocatalyst

Yao *et al.* (2004) also studied the effect of calcination time on the photocatalytic activity of the prepared bismuth titanate photocatalyst thin film calcined at 600 °C. The results showed that at 1 min of calcination time, the highest decomposition of methyl orange was obtained. While the rate constant increased with increasing calcination temperature, but at calcination time of 5 min, the rate constant reached the highest value because at the higher calcination time of 10 min, the sintering of photocatalyst material occurred.

2.7 Porous Materials

The classification of pores according to size has been under discussion for many years, but in the past, the terms ''micropore'' and ''macropore'' have been applied in different ways by physical chemists and some other scientists. In an attempt to clarify this situation, the limits of size of the different categories of pores included in Table 2.3 have been proposed by the International Union of Pure and Applied Chemistry (IUPAC) (Ishizaki *et al.*, 1988 and Rouquerol *et al.*, 1999). As indicated, the ''pore size'' is generally specified as the ''pore width'', i.e. the available distance between the two opposite walls. Obviously, pore size has a precise meaning when the geometrical shape is well defined. Nevertheless, for most purposes, the limiting size is that of the smallest dimension, and this is generally

taken to represent the effective pore size. Micropores and mesopores are especially important in the context of adsorption.

Table 2.3 Definitions about porous solids.

Term	Definition
Porous solid	Solid with cavities or channels which are deeper than they are wide
Micropore	Pore of internal width less than 2 nm
Mesopore	Pore of internal width between 2 and 50 nm
Macropore	Pore of internal width greater than 50 nm
Pore size	Pore width (diameter of cylindrical pore or distance between opposite walls of slit)
Pore volume	Volume of pores determined by stated method
Surface area	Extent of total surface area determined by given method under stated conditions

According to the IUPAC classification, porous materials are regularly organized into three categories on a basis of predominant pore size as follows:

- Microporous materials (pore size < 2 nm) include amorphous silica and inorganic gel to crystalline materials, such as zeolites, aluminophosphates, gallophosphates, and related materials.
- Mesoporous materials (2 nm ≤ pore size ≤ 50 nm) include the M41S family (e.g. MCM-41, MCM-48, MCM-50, etc.) and other non-silica materials synthesized via intercalation of layered materials, such as double hydroxides, metal (titanium, zirconium) phosphates, and clays.
- Macroporous materials (pore size > 50 nm) include glass-related materials, aerogels, and xerogels.

Nowadays, micro- and mesoporous materials are generally called nanoporous materials''. Particularly, mesoporous materials are remarkably very

suitable for catalysis applications, whereas the pores of microporous materials may become easily plugged during catalyst preparation if high metal loading is required.

2.8 Sol-Gel Process

The sol-gel process has been intensively studied because it is so effective to prepare nano-sized mesoporous materials (Sreethawong *et al.*, 2005). Because the metal oxides can be deactivated due to sintering or crystal growth during their continuous use in high temperature processes, and the photocatalytic performance of the metal oxides is well-known to depend on their specific surface area, sol-gel method presents some particular advantages through a low-temperature process, avoiding contamination of the materials. It also yields better stoichiometric control and the possibility of grain-size and grain-shape control. This technique does not require complicated instruments, such as in chemical vapor deposition method. It provides a simple and easy means of synthesizing nano-sized particles, which is essential for nano-photocatalysts. It involves the formation of metal-oxo-polymer network from molecular precursors, such as metal alkoxides, and subsequent polycondensation, as follows:

$$\text{M-OR} + \text{H}_2\text{O} \rightarrow \text{M-OH} + \text{ROH} \quad (20)$$

$$\text{M-OH} + \text{M-OR} \rightarrow \text{M-O-M} + \text{R-OH} \quad (21)$$

$$\text{M-OH} + \text{M-OH} \rightarrow \text{M-O-M} + \text{H}_2\text{O} \quad (22)$$

where M = Ti, Si, Zr, Al, and R = alkyl group.

All stages, including the formation of colloid particles to form gel network, drying of wet gel, and calcination stage, can all lead to grain growth and formation of agglomerates. Hence, to carefully control the process is very essential in preparing high-performance and high-reliability powders. The relative rates of hydrolysis and polycondensation strongly influence the structure and properties of the resulting metal oxides. Typically, sol-gel-derived precipitates are amorphous in nature, requiring further heat treatment to induce crystallization. The calcination process frequently gives rise to particle agglomeration and grain growth, and may induce phase transformation (Wang and Ying, 1999). Thus, a surfactant is used to prevent agglomeration of the particle. The $BaTiO_3$ nanoparticles synthesized by sol-gel

process (Yu *et al.*, 2008), however, are easy to form agglomeration. This can be avoided by the application of the surfactant, i.e. oleic acid, as cheap and innoxious surfactant, thus preventing the agglomeration of particles. The sol-gel process by the addition of surfactant can help enforce size controllability and prepare well-dispersed powders. The ideal model of forming the $BaTiO_3$ is shown in Figure 2.5 .

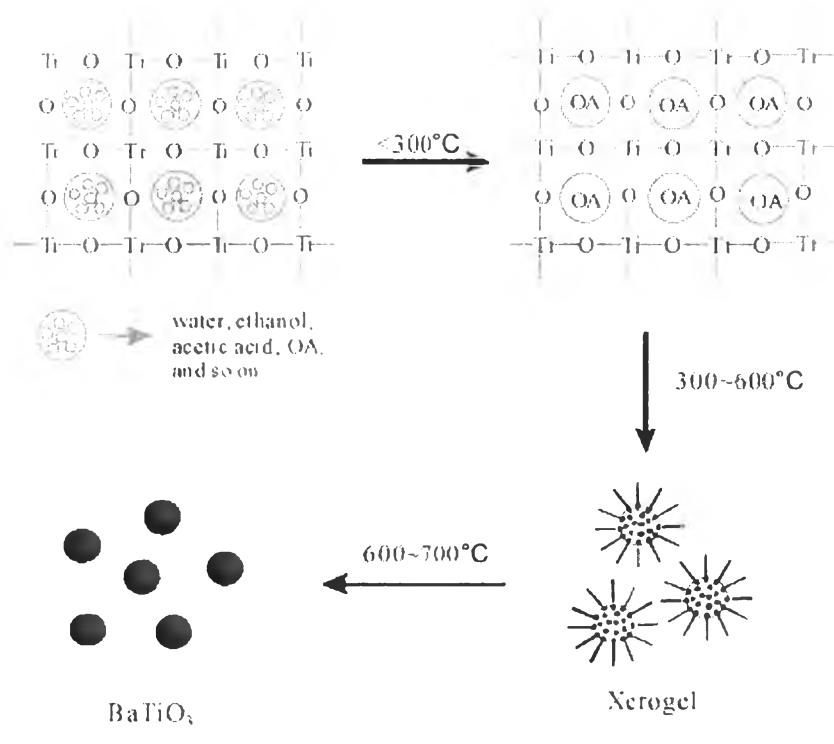

Figure 2.5 A schematic of forming the $BaTiO_3$ nanoparticles (Yu *et al.*, 2008).

The process can be divided to three steps. Firstly, oleic acid (OA) enchases in the 3D network structure of -Ti-O-Ti- when the temperature is lower than 300°C. Secondly, between 300 and 600 °C, a number of "microcapsules" of $BaTiO_3$ precursors coated by OA are formed. The carboxyl of OA is towards the inside and hydrophobic -R group towards the outside. Excessive OA as solution will allow the system to form "microcapsules". Finally, when the temperature is higher than 600 °C, OA decomposes, and the walls of "microcapsules" are destroyed. Although this happens, the shape of $BaTiO_3$ precursor is preserved, thus producing better-dispersed $BaTiO_3$ nanoparticles.

Factors affecting the sol-gel process include the reactivity of metal alkoxides, pH of the reaction medium, water-to-alkoxide ratio, reaction temperature, and nature of solvent and additive. The water-to-alkoxide ratio governs the sol-gel chemistry and the structural characteristics of the hydrolyzed gel. High water-to-alkoxide ratio in the reaction medium ensures a more complete hydrolysis of alkoxides, favoring nucleation versus particle growth. In addition, an increase in water-to-alkoxide ratio leads to reducing the crystallite size of the calcined catalyst. An alternative approach to control the sol-gel reaction rates involves the use of acid or base catalyst. It was reported that for a system with a water-to-alkoxide ratio of 165, the addition of HCl resulted in the reduction of the crystallite size from 20 to 14 nm for materials calcined at 450 °C. Besides, a finer grain size and a narrower pore size distribution with a smaller average pore diameter were also attained for the sample synthesized with HCl (Wang and Ying, 1999). The size of alkoxide group also plays an important role in controlling the particle size. The titanium alkoxide containing bulky groups, such as titanium amiloxide, reduces the hydrolysis rate, which is advantageous for the preparation of fine colloidal particles (Murakami *et al.*, 1999).